

Flow through a rotating helical pipe with a wide range of the Dean number

M.M. ALAM¹⁾, M. OTA²⁾, M. FERDOWS²⁾, M.N. ISLAMV³⁾,
M. WAHIDUZZAMAN⁴⁾, K. YAMAMOTO⁴⁾

¹⁾ *Mathematics Discipline, Khulna University
Khulna-9208, Bangladesh*

²⁾ *Department of Mechanical Engineering,
Tokyo Metropolyton University, Tokyo, Japan*

³⁾ *Department Mathematics, Chittagong University of Engineering Technology,
Chittagong, Bangladesh*

⁴⁾ *Department of Mechanical Engineering,
Okayama University, Okayama, Japan*

THE INCOMPRESSIBLE VISCOUS steady flow through a helical pipe of circular cross-section rotating at a constant angular velocity about the center of curvature is investigated numerically to examine the combined effects of rotation (Coriolis force), torsion and curvature (centrifugal force) on the flow. The flow depends on the Taylor

number $T_r = \frac{2a^2\Omega_T}{v} \sqrt{\frac{2}{\delta + 2\beta_0^2}}$, the Dean number $D_n = \frac{\sqrt{2\delta}a^3G}{\mu v}$, the torsion para-

meter $\beta_0 = \frac{\lambda}{\sqrt{2\delta}}$ and the dimensionless curvature of the duct δ , where a is the radius of the helical pipe, Ω_T the angular velocity, μ the viscosity, v the kinematic viscosity, G the constant pressure gradient along the pipe axis and β_0 – a parameter related to the torsion τ and curvature δ . When $\Omega_T > 0$, the rotation is in the direction in which the Coriolis force produces the curvature effect. When $\Omega_T < 0$, the rotation is in the direction in which the Coriolis force exhibits an opposite effect to that of curvature. The calculations are carried out for $-500 \leq T_r \leq 500$, $1500 \leq D_n \leq 2000$ (large Dean number), $0 \leq \beta_0 \leq 0.4$ and $0 < \delta \leq 0.2$. The total flux through the duct has a sharp peak at a negative T_r .

1. Introduction

THE FLOW THROUGH a curved tube has attracted considerable attention not only because of its practical importance in chemical and mechanical engineering, but also because of the physically interesting features under the action of centrifugal force caused by curvature of the tube. DEAN [6] was the pioneer of the problem in mathematical terms under the fully developed flow condition. He

found the secondary flow consisting in a pair of counterrotating vortices caused by the centrifugal force. Since then, the secondary flow driven by the centrifugal force in a curved pipe has been studied extensively, as shown in the review articles by BERGER TALBOT and YAO [1], NANDAKUMAR and MASLIYAH [16] and ITO [9]). The fluid flowing through a tube rotating at a constant angular velocity about an axis normal to a plane including the tube is subject to both the Coriolis and centrifugal forces. Such rotating passages are used in cooling systems for conductors of electric generators.

Flow in a rotating straight duct is of interest because the secondary flows in this case are qualitatively similar to those in stationary curved systems in view of the similar centrifugal mechanisms inducing the secondary flows in the two systems (ISHIGAKI [11]). Since the pipelines have more or less bent or curved sections, it is interesting to investigate the combined effects of curvature and rotation, which are relevant to the flow in rotating curved ducts. MIYAZAKI [15] examined the solutions when the pressure-driven flow proceeds in the same direction of rotation. This is called the co-rotating case. ITO and MOTAI [9] investigated both co-rotating and counter-rotating cases with respect to the direction of pressure-driven flow. A reduction in the strength of the secondary flow and even a secondary flow reversal was observed for counter rotating case. Moreover, DASKOPOULOS and LENHOFF [5] showed the bifurcation study of the flow combined with curvature and rotation. The above-mentioned works have been considered for a circular cross-section.

The curved geometry of helical pipe is important from both-industrial and academic standpoint. The helical pipe has been used extensively in various industrial applications to enhance the rate of heat, mass and momentum transfer. In order to improve the performance of these devices, an accurate and reliable analysis of the flow in the helical pipe is necessary. These devices could also be used as a basis for studying the flow in other devices, such as screw pumps, heat exchangers and the passage between the blades of gas turbines or centrifugal compressors. The shape of a helical pipe, as shown in Fig. 1a, is determined by the dimensionless curvature δ and torsion λ . The torsion and curvature are defined, respectively, as $\lambda = \frac{ab'}{b'^2 + c'^2}$ and $\delta = \frac{ac'}{b'^2 + c'^2}$, where a is the radius of the cross-section of the helical pipe, $2\pi b'$ the pitch of the helical pipe, and c' , the radius of the helix of the center-line of the helical pipe. The curvature δ and torsion λ of the center-line of the pipe characterize the particular kind of a pipe. For example, for a toroidal pipe, δ is constant and λ is zero, and for helical pipe, both λ and δ are constant and nonzero. The torsion gives rise to the so-called pitch of the duct, $2\pi b'$, as shown in Fig. 1a. WANG [20] for the first time handled the problem of flow in a helical circular duct using a non-orthogonal, helical co-ordinate system. The flow in the helical pipe has been studied for cir-

cular (MANLAPAZ *et al.* [14] WANG [20] MURATA *et al.* [16] GERMANO [7], CHEN and FAN [2], KAO [12], XIE [19], TUTTLE [18], CHEN and JAN [3]) and elliptical (GERMANO [8]) cross-sections. The previous theoretical studies mentioned above are limited to small curvature and torsion. LIU and MASLIYAH [13] numerically solved the problem of laminar flows in a circular pipe having a non-zero pitch. They discussed in detail secondary flow patterns in a cross-section of the pipe. However, their analysis is limited to a small Dean number and small curvature. YAMAMOTO *et al.* [22] investigated numerically the flow through a helical pipe for a wide range of the Dean number, curvature and torsion. They employed the orthogonal coordinate system and solved the equations numerically by applying the spectral method. YAMAMOTO *et al.* [23] also conducted experiments on the flow in helical circular tube over a range of Reynolds numbers from about 500 to 2000. The results reveal a rather large effect of torsion on the flow. Quite recently, YAMAMOTO, MAHMUD ALAM, YASUHARA and ARIVOWO [24] studied the helical pipe flow with rotation for a small range of Dean number. For a wide range of the Dean number, curvature and torsion, no work regarding the helical pipe flow with rotation has been done. In this respect, it is quite innovative to investigate the flow in a rotating helical pipe for a wide range of the Dean number, curvature and torsion to understand the flow behavior. This is the main objective of the present paper.

2. Governing equations

We have considered the coordinate system (s', r', θ') as shown in Fig. 1b for fully a developed flow in a rotating helical circular pipe. In this figure, s' is the coordinate along the center-line of the duct, \mathbf{T} – the unit tangent vector along s' , and \mathbf{N} and \mathbf{B} – the normal and binormal vectors, respectively. The right-handed helix is considered in our work (see Fig. 1a). The angle ϕ is defined by

$$(2.1) \quad \phi(s') = \int_{s'_0}^{s'} \tau'(s) ds$$

where τ' is the torsion of the center-line of the pipe and s'_0 is arbitrary as long as $s' \geq s'_0$. Variables are non-dimensionalized by using a , the radius of the circular tube, ν the kinematic viscosity and ρ the density of the fluid. We introduce the non-dimensional variables defined by:

$$(2.2) \quad \begin{aligned} r &= \frac{r'}{a}, & u &= \frac{a}{\nu} u', & v &= \frac{a}{\nu} v', & w &= \frac{a}{\nu} w' \sqrt{2\delta}, \\ \delta &= \frac{a}{L}, & \lambda &= a\tau', & p &= \left(\frac{a}{\nu}\right)^2 \frac{p'}{\rho}, & s &= \frac{s'}{a}. \end{aligned}$$

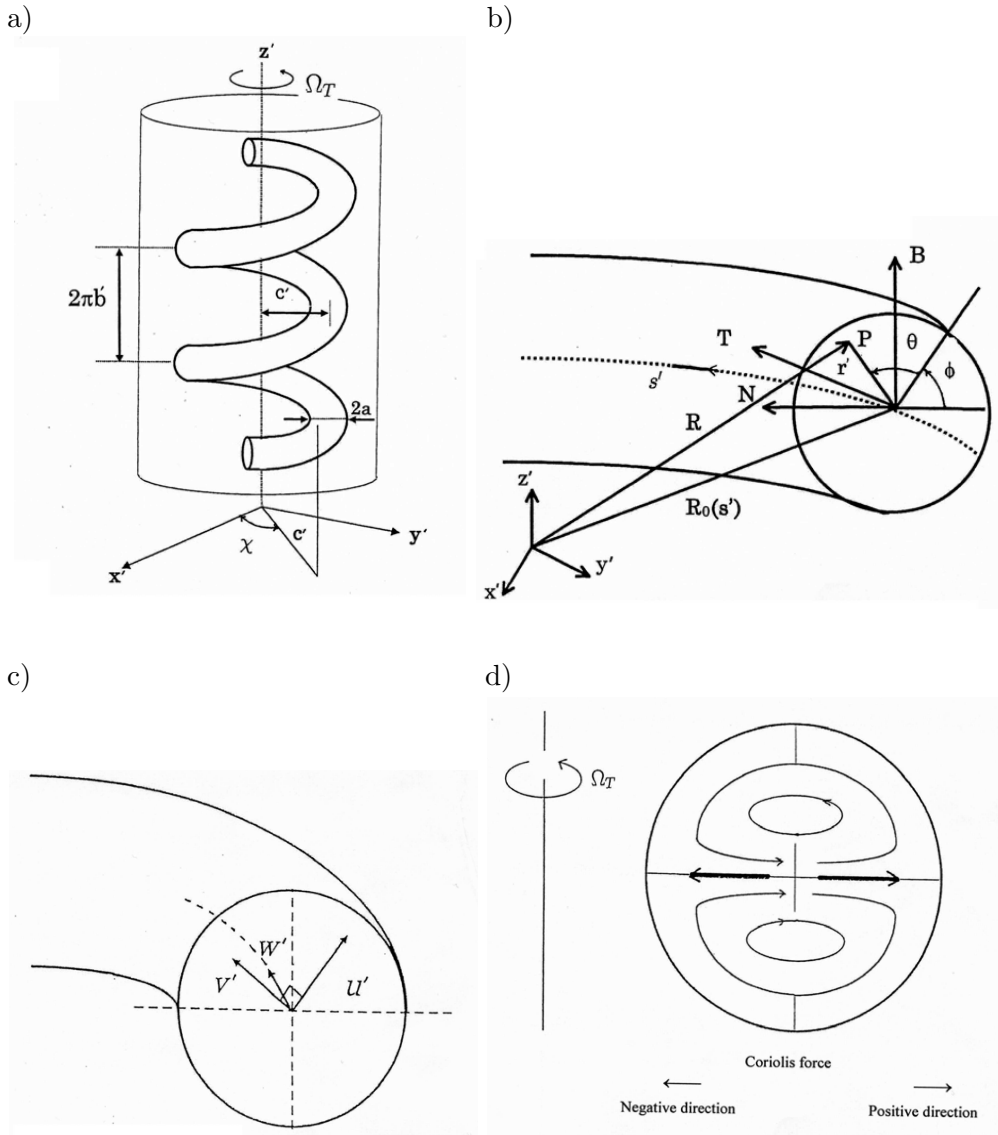


FIG. 1. a) Helical pipe with circular cross-section; b) Co-ordinate system; c) The directions of the u' , v' and w' velocity components; d) Geometrical configuration.

Here u , v and w are the velocity components in the r , α , s directions respectively and these are shown in Fig. 1c, p is the pressure, δ the non-dimensional curvature, λ the non-dimensional torsion and the variables with prime are dimensional quantities. With reference to the generalized equations, the Navier–Stokes

equations can be put mathematically in the following non-dimensional forms:

$$(2.3) \quad \frac{1}{r} \frac{\partial}{\partial r}(ru) + \frac{1}{r} \frac{\partial v}{\partial \alpha} + \frac{\beta_0}{\omega} \frac{\partial w}{\partial \alpha} + \frac{\delta}{\omega}(u \cos \alpha - v \sin \alpha) = 0,$$

$$(2.4) \quad Du - \frac{v^2}{r} - \frac{\cos \alpha}{\omega} \frac{w^2}{2} + \frac{1}{2} T_r (2\beta_0 v - w \cos \alpha) = -\frac{\partial p_1}{\partial r} \\ - \left(\frac{1}{r} \frac{\partial}{\partial \alpha} - \frac{\delta \sin \alpha}{\omega} \right) \Omega + \frac{\beta_0}{\omega} \frac{\partial}{\partial \alpha} \left(\frac{2\delta\beta_0}{\omega} \frac{\partial u}{\partial \alpha} - \frac{\partial w}{\partial r} - \frac{\delta \cos \alpha}{\omega} w \right),$$

$$(2.5) \quad Dv + \frac{uv}{r} + \frac{\sin \alpha}{\omega} \frac{w^2}{2} + \frac{1}{2} T_r (w \sin \alpha - 2\beta_0 u) = -\frac{1}{r} \frac{\partial p_1}{\partial \alpha} \\ + \left(\frac{\partial}{\partial r} + \frac{\delta \cos \alpha}{\omega} \right) \Omega + \frac{\beta_0}{\omega} \frac{\partial}{\partial \alpha} \left(\frac{2\delta\beta_0}{\omega} \frac{\partial v}{\partial \alpha} - \frac{1}{r} \frac{\partial w}{\partial \alpha} + \frac{\delta \sin \alpha}{\omega} w \right),$$

$$(2.6) \quad Dw + \frac{\delta \cos \alpha}{\omega} uw - \frac{\delta \sin \alpha}{\omega} vw + T_r \delta (u \cos \alpha - v \sin \alpha) = \frac{D_n}{\omega} \\ - \frac{2\delta\beta_0}{\omega} \frac{\partial p_1}{\partial \alpha} + \frac{1}{r} \frac{\partial}{\partial r} r \left(\frac{\partial w}{\partial r} + \frac{\delta w \cos \alpha}{\omega} - \frac{2\delta\beta_0}{\omega} \frac{\partial u}{\partial \alpha} \right) \\ - \frac{1}{r} \frac{\partial}{\partial \alpha} \left(\frac{2\delta\beta_0}{\omega} \frac{\partial v}{\partial \alpha} - \frac{1}{r} \frac{\partial w}{\partial \alpha} + \frac{\delta \sin \alpha}{\omega} w \right),$$

where Ω , ω , D and α are defined by

$$(2.7) \quad \Omega = \frac{\partial v}{\partial r} + \frac{v}{r} - \frac{1}{r} \frac{\partial u}{\partial \alpha}, \quad \omega = 1 + \delta r \cos \alpha, \\ D = u \frac{\partial}{\partial r} + \frac{v}{r} \frac{\partial}{\partial \alpha} + \frac{\beta_0}{\omega} w \frac{\partial}{\partial \alpha}, \quad \alpha = \theta + \phi.$$

The pressure can be written in the form

$$(2.8) \quad p = -\frac{D_n s}{\sqrt{2\delta}} + p_1(r, \alpha) + \frac{T_r^2}{16} (\delta + 2\beta_0^2) \left[\left(\frac{c}{a} + r \cos \alpha \right)^2 + 2\beta_0^2 \frac{c}{a} \sin^2 \alpha \right],$$

where p_1 is the deviation of the pressure in a cross-section and G is a constant representing the pressure gradient along the pipe center-line. The non-dimensio-

nal parameters T_r (Taylor number), D_n (Dean number) and β_0 (torsion parameter) were defined earlier. Considering the continuity Eq. (2.3), we can introduce the modified stream function ψ which is related to u, v and w by

$$(2.9) \quad u = \frac{1}{r\omega} \frac{\partial \psi}{\partial \alpha}, \quad v = -\frac{1}{\omega} \frac{\partial \psi}{\partial r} - \frac{\beta_0 r}{\omega} w.$$

Putting this equation into Eqs. (2.4)–(2.6) and eliminating p_1 in the resulting relations, we get the equations for w and ψ . The relations for w and ψ are actually used for numerical computations and these are not shown for brevity. The boundary conditions at the wall surface are given by

$$(2.10) \quad w = u = v = 0, \quad \text{or} \quad w = \psi = \frac{\partial \psi}{\partial r} = 0 \quad \text{at} \quad r = 1.$$

3. Flux through the rotating helical pipe

The dimensional mean axial velocity \bar{w}' is expressed by

$$(3.1) \quad \bar{w}' = \frac{1}{\pi a^2} \int_0^a r' dr' \int_0^{2\pi} w' d\alpha = \frac{v}{2a} \frac{k}{\sqrt{\delta}},$$

where

$$k = \frac{\sqrt{2}}{\pi} \int_0^1 r dr \int_0^{2\pi} w d\alpha$$

is the dimensionless flux.

We define the non-dimensional mean radial velocity \bar{w} as

$$(3.2) \quad \bar{w} = \frac{a}{v} \bar{w}' = \frac{k}{2\sqrt{\delta}}.$$

The flux of the rotating helical pipe Q_c and that of a straight tube Q_s are given by

$$(3.3) \quad Q_c = \pi a^2 \bar{w}' = \frac{\pi}{2} a v \frac{k}{\sqrt{\delta}},$$

$$(3.4) \quad Q_s = \frac{\pi G a^4}{8\mu}.$$

Therefore, we have

$$(3.5) \quad \frac{Q_c}{Q_s} = \frac{4\sqrt{2k}}{D_n}.$$

We define the Reynolds number as

$$(3.6) \quad R_e = \frac{\overline{w}'(2a)}{v} = \frac{k}{\sqrt{\delta}}.$$

4. Method of numerical calculation

The numerical calculation technique corresponds exactly to those given by YAMAMOTO, MD. MAHMUD ALAM, YASUHARA and ARIVOWO [24] and so their description are not reproduced here for brevity. We will present here only the basic concept of the numerical calculation technique. The spectral method is applied in the numerical calculation. The Fourier series are used for the circumferential direction α and the series of the Chebyshev polynomials in the radial direction r . That is, we expand ψ and w as

$$(4.1) \quad w(r, \alpha) = \sum_{n=1}^N w_n^s(r) \sin(n\alpha) + \sum_{n=0}^N w_n^c(r) \cos(n\alpha),$$

$$\psi(r, \alpha) = \sum_{n=1}^N f_n^s(r) \sin(n\alpha) + \sum_{n=0}^N f_n^c(r) \cos(n\alpha),$$

where N is the truncation number of the Fourier series. The collocation points are taken as

$$(4.2) \quad R = \cos \left\{ \frac{M+2-i}{M+2} \right\} \pi \quad (1 \leq i \leq M+1).$$

The obtained algebraic non-linear equations are solved by an iteration method with under-relaxation. Convergence of the solution is assured by taking $\epsilon_p < 10^{-5}$, where subscript p denotes the iteration number.

5. Results and discussion

The main flow is forced by the pressure gradient along the centerline of the pipe. The helical tube is rotating around the center of curvature of the duct with angular speed Ω_T . According to the definition of T_r , a positive T_r means that the duct rotates in the same sense as the movement with axial velocity of the fluid within the pipe and we call this with co-rotation (see Fig. 1d). On the other hand, the negative T_r is the case when the helical duct rotates in the opposite sense with respect to the axial velocity, and this is called the

counter-rotation (see Fig. 1d). YAMAMOTO, MD. MAHMUD ALAM, YASUHARA and ARIVOWO [24] have studied the present problem for a small range of Dean numbers ($D_n = 500$ and 1000). In the present problem, numerical calculations have been made of a wide range of the Dean numbers ($D_n = 1500$ and 2000) for two cases of curvature δ , 0.01 and 0.2 , the Taylor numbers T_r ranging from -500 to 500 , and the torsion parameter $\beta_0 = 0.4$. The truncation number was taken to be $M = 35$ and $N = 60$ with good accuracy. The obtained results in this matter are presented below.

5.1. Variation of the flux and the flow behavior with rotation

First, we describe the variation of the flux and the flow velocity with rotation at the Dean number 1500 and 2000 . The curvature δ is taken to be 0.01 and 0.2 . The torsion parameter β_0 is kept constant and equal to 0.4 .

CASE 1. $D_n = 1500$.

Figure 2 shows the flux ratio $\frac{Q_c}{Q_s}$ (where Q_s is the flux through the straight tube and Q_c the flux through the rotating helical pipe (at the same pressure gradient G) through the pipe versus the Taylor number T_r at $\delta = 0.01$ and 0.2 and $\beta_0 = 0.4$. The figure indicates that the flux increases as T_r decreases from zero and it has a sharp peak close to the points where $T_r = -270$ for $\delta = 0.01$ and $T_r = -275$ for $\delta = 0.2$. Actually we are not able to obtain the flux near

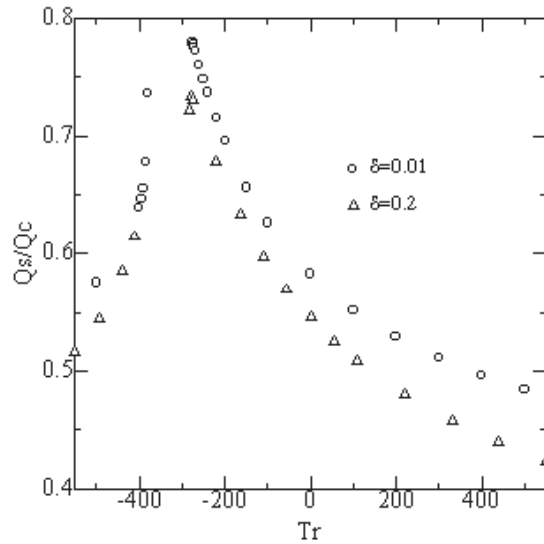


FIG. 2. State diagram in terms of the dimensionless flux ratio Q_c/Q_s versus the Taylor number T_r , for the flow through a rotating helical pipe of circular cross-section at Dean number $D_n = 1500$, with $\beta_0 = 0.4$.

the peak point(at the left side) because the convergence of the solution in the numerical calculation is very poor in that region. After that, the flux decreases as T_r further decreases. The flux of $\delta = 0.01$ is larger than that of $\delta = 0.2$. It is well understood that the high-curvature pipe makes the secondary flow strong and for the fluid is not easy to flow. It is interesting to notice that the peaks of the flux for two cases of curvature occur at about the same T_r and the neighbouring flux ratios. Also the peaks are to be found to be near the unity.

There are large differences between the fluxes at large $|T_r|$ in two cases. We shall depict the flow structures at several points of T_r in Fig. 3a–k when $\delta = 0.01$.

Here and in the following figures, the left-hand figures show the vector plots of the secondary flow in a cross-section, while the equi-velocity lines of the axial flow are shown in the right-hand figures. The view from the upstream of the pipe is shown in the figures. In this section, the increment of the axial velocity is 30. The outer wall, i.e., the N direction, is to the right. The length of arrow indicates the ratio of the stream velocity to the mean axial velocity and the direction of the flow in vector plots are always indicated by an arrow-head, no matter how small the flow is. The middle figures show the constant line of ψ and the increment of ψ is 1.5. Therefore, from this figure we can understand the secondary convection of fluid particles in a cross-section of the pipe. The vector plots and the axial velocity contour plots are quantities which are measurable experimentally by a pointing device, e.g. a hot-wire anemometer. It is seen in some cases, e.g. in Fig. 3g, that there is a difference in the flow pattern between constant ψ lines and vector plots.

We shall discuss the variation of the flow behavior with T_r by mainly using constant ψ lines. A pair of vortices located at the upper left, and lower left, with unequal size but opposite direction of rotation, is shown in Fig. 3f at $T_r = 0.0$. The vortex rotating in the counter-direction of torsion (the upper vortex rotating anti-clockwise) is larger and appears at the upper left of the cross-section. On the other hand, the other vortex rotating in the same direction of torsion (lower vortex rotating clockwise) is a little smaller and appears at the lower right of the cross-section (see Fig. 3c). This figure also shows the location of the maximum axial velocity being at upper right of the cross-section. Now we decrease T_r to the point where $T_r = -100$. The flow pattern at this point is shown in Fig. 3g. It will be seen that the previous two vortices become an almost single vortex. The center of the vortex moves to the upper left of the cross-section. If we further decrease the value of T_r to the point where $T_r = -275$ and the flux ratio has almost its peak, the secondary flow shows an interesting feature (see Fig. 3i). Almost the only one vortex of the secondary flow is observed and it is stronger near the centre of the cross-section. The velocity near the wall is very weak.

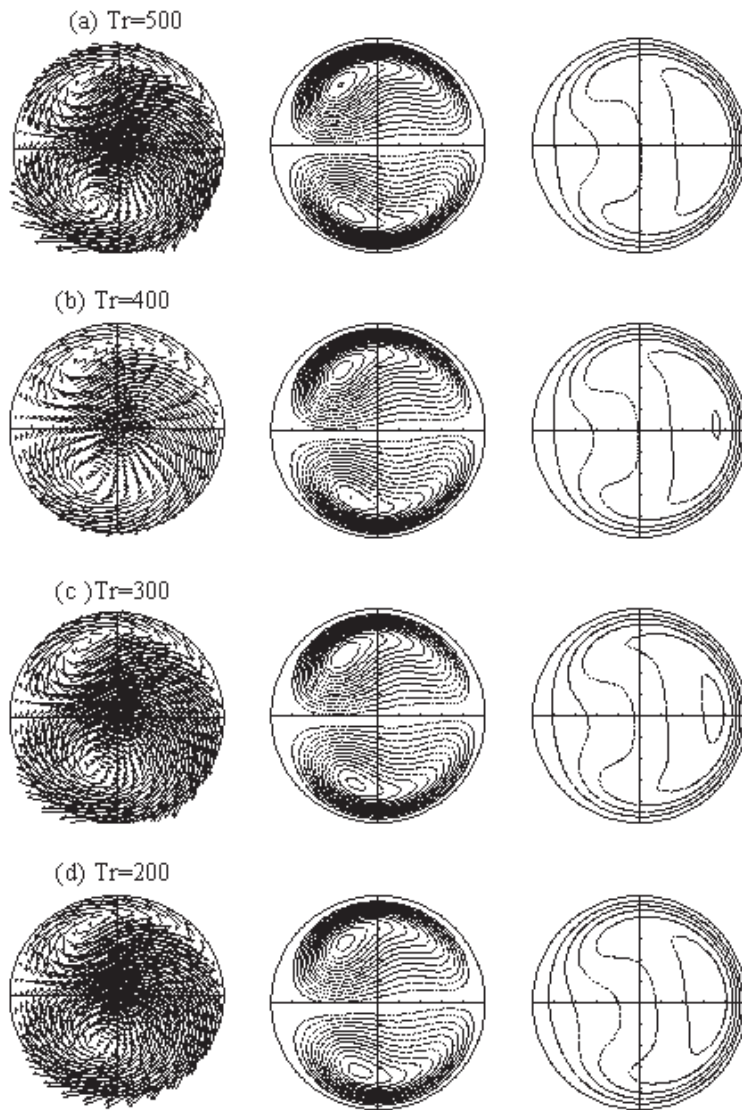


[FIG. 3a-d]

The centre of the maximum axial flow is close to the centre of the cross-section. This means that at the peak point the axial flow pattern approaches that of the ordinary Poiseuille flow.

In this region of the Taylor number, the Coriolis force almost equals the centrifugal force. If we further increase $|T_r|$ to negative value from the peak point of the flux, then we find that the flux suddenly decreases. That is, the

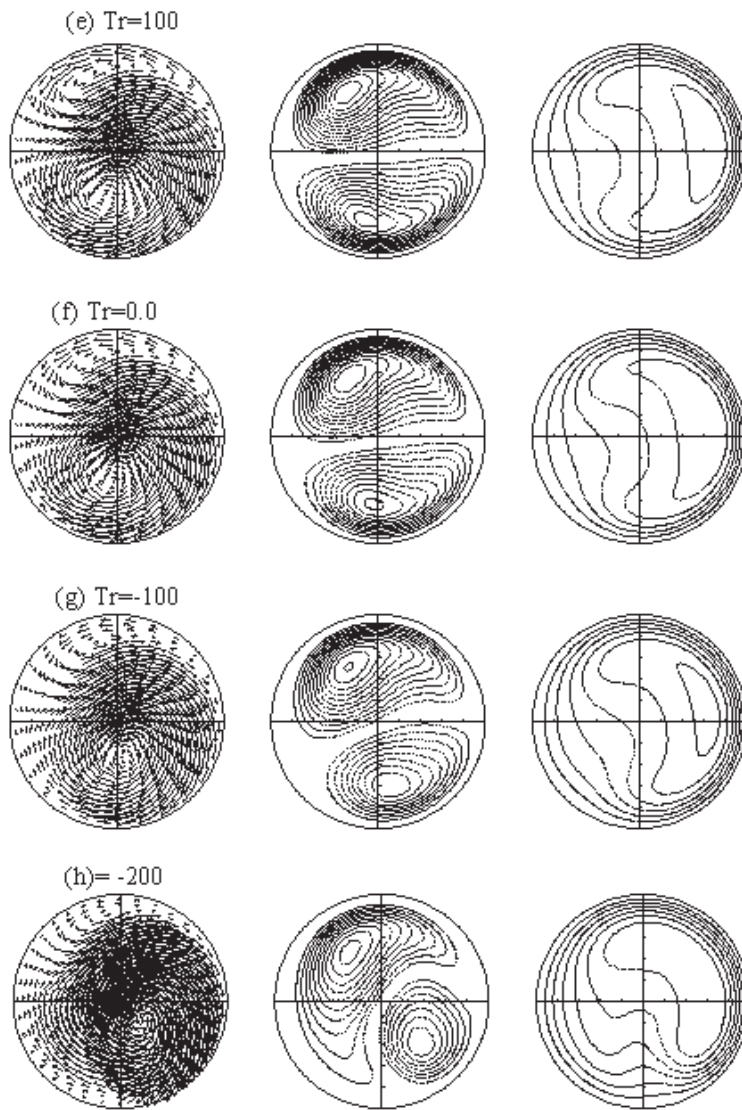


[FIG. 3e-h]

flux has a sharp peak. The flow pattern after the peak point (where $T_r = -400$) is shown in Fig. 3j. It is seen from this figure that its one weak vortex starts to develop near the upper wall of the cross-section. The main vortex occupies most area of the cross-section, and these two vortices are of reversed type as compared with Fig. 3f. The maximum axial velocity is shifted to the lower left of the cross-section. Further if we decrease the value of T_r to -500 (see Fig. 3),

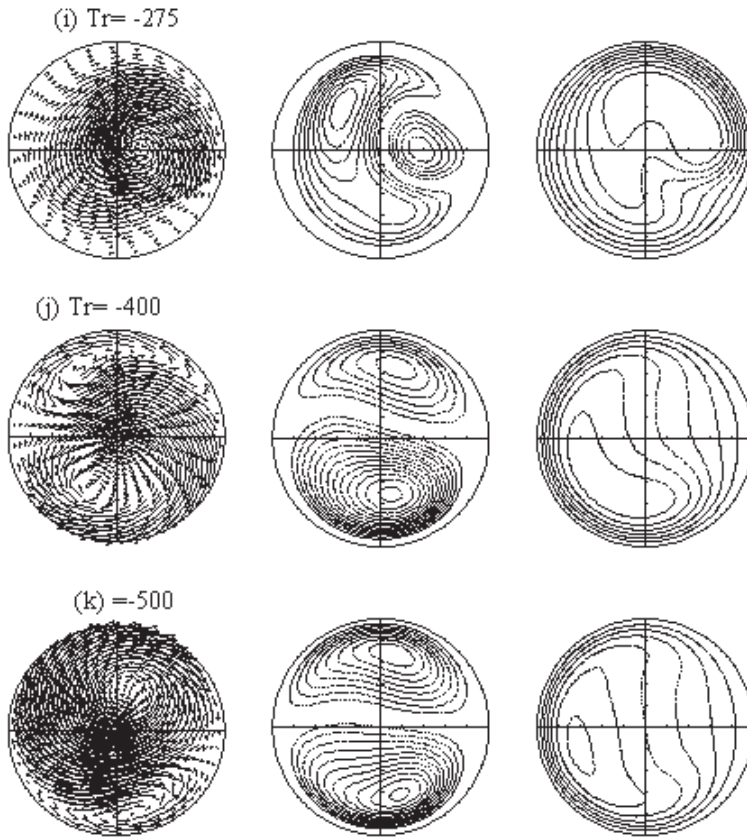


FIG. 3. (i–j) Vector plots of the secondary flow (left), stream-lines of the secondary flow (middle) and contour plots of the axial flow (right) through the rotating helical pipe at different values of T_r in case of $D_n = 2000$, with $\beta_0 = 0.4$ and $\delta = 0.01$.

we get again two vortices of almost equal size. The flow is completely reversed as compared with the flow of $T_r = 0.0$ (see Fig. 3f).

The physical mechanism responsible for such a behavior is easily understood once we recognize that without rotation and torsion, the curvature has the tendency to induce a secondary flow directed radially outwards in the middle of the channel, while without torsion the system rotation has a tendency to induce a secondary flow in radially inward direction. The center of the maximum axial flow (see Fig. 3k) has been approximately shifted to the opposite side as compared to Fig. 3c where $T_r = 500$.

We next proceed to the discussions concerning the co-rotation. Starting from the point where $T_r = 0$ (see Fig 3f) and increasing T_r , we reach the point where

$T_r = 500$. The flow structure at this point is shown in Fig. 3e–a. It will be seen that there is no qualitative difference with the flow structure of $T_r = 0$ (Fig. 3f). At $T_r = 500$, the secondary flow as well as axial flow behavior are almost the same as the flow behavior at $T_r = -500$, but of reversed type. This is due to the Coriolis force added to the centrifugal force.

CASE 2. $D_n = 2000$.

Figure 4 shows variation of the flux ratio with the Taylor number T_r when $D_n = 2000$, $\delta = 0.01$ and 0.2 , and $\beta_0 = 0.4$. In the present cases, we are not able to obtain the flux near the peak point because the convergence of the solution in the numerical calculation is very poor in that region. However, we will see that the flux at a higher Dean number has a lower value at a constant Taylor number. The presumed peak point moves to a lower value of T_r (higher $|T_r|$) for larger Dean numbers. It will be seen that the flux has a sharp peak at larger value of $|T_r|$ as compared with that of $D_n = 500$ (YAMAMOTO, MD. MAHMUD ALAM, YASUHARA and ARIVOWO [24]).

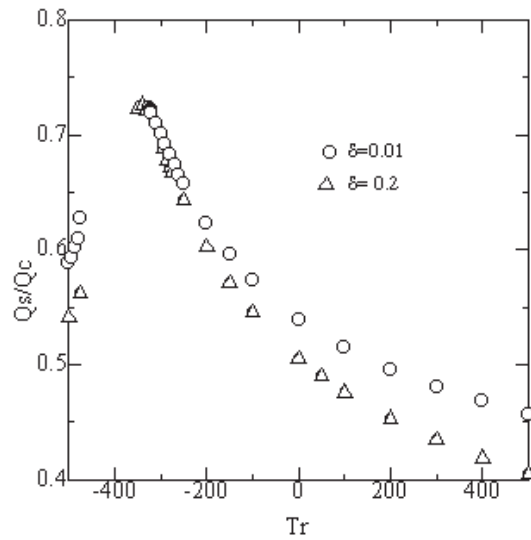
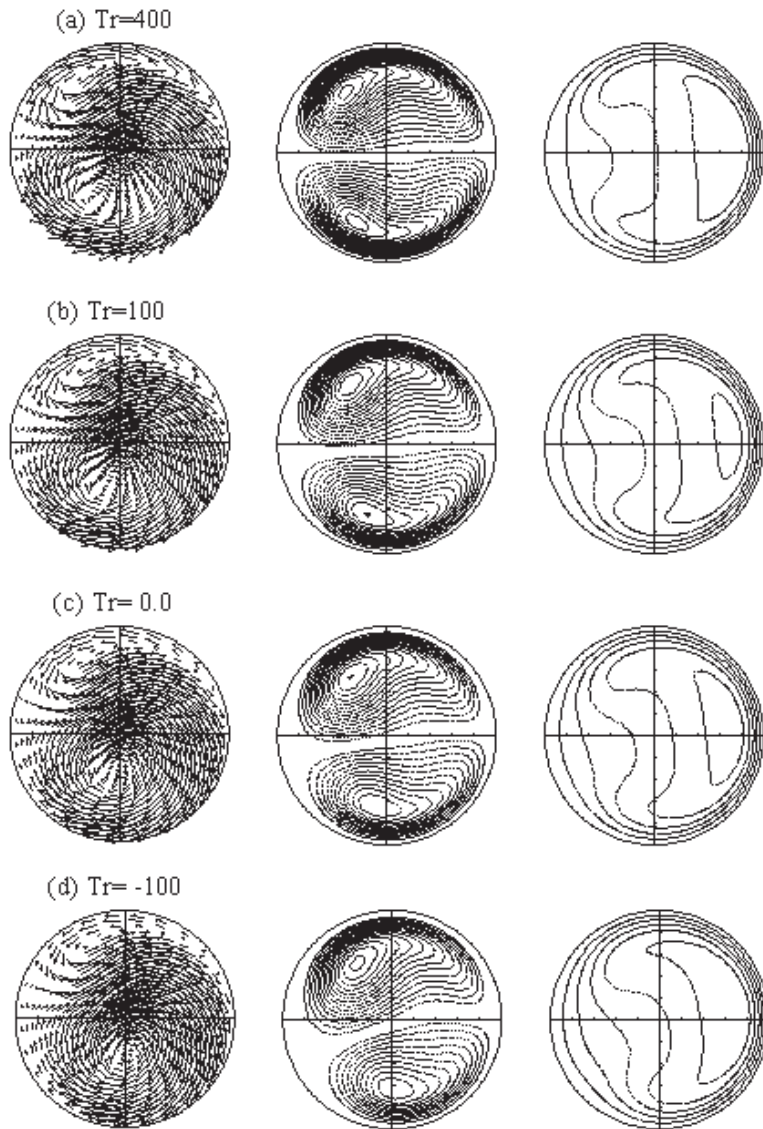


FIG. 4. State diagram in terms of the dimensionless flux ratio Q_c/Q_s versus the Taylor number T_r , for the flow through a rotating helical pipe of circular cross-section at Dean number $D_n = 2000$, with $\beta_0 = 0.4$.

The effect of the centrifugal force is larger at larger flow rate, i.e., larger D_n , without rotation. We need a large negative Coriolis force, i.e. large T_r , to counter-balance the large centrifugal force. The strong secondary flow caused by a large centrifugal force also makes the fluid difficult to flow. This is responsible for lower

value of the flux, compared to that of $D_n = 500$ (YAMAMOTO, MD. MAHMUD ALAM, YASUHARA AND ARIVOWO [24]). Fig. 5a–g shows the flow structure. In this figure, the increment of the axial velocity is 40 and the increment of the ψ is 2.0. Variation of the flow behavior with the Taylor number introduces no significant qualitative changes as compared to the previous case of $D_n = 1500$.



[FIG. 5a–d]

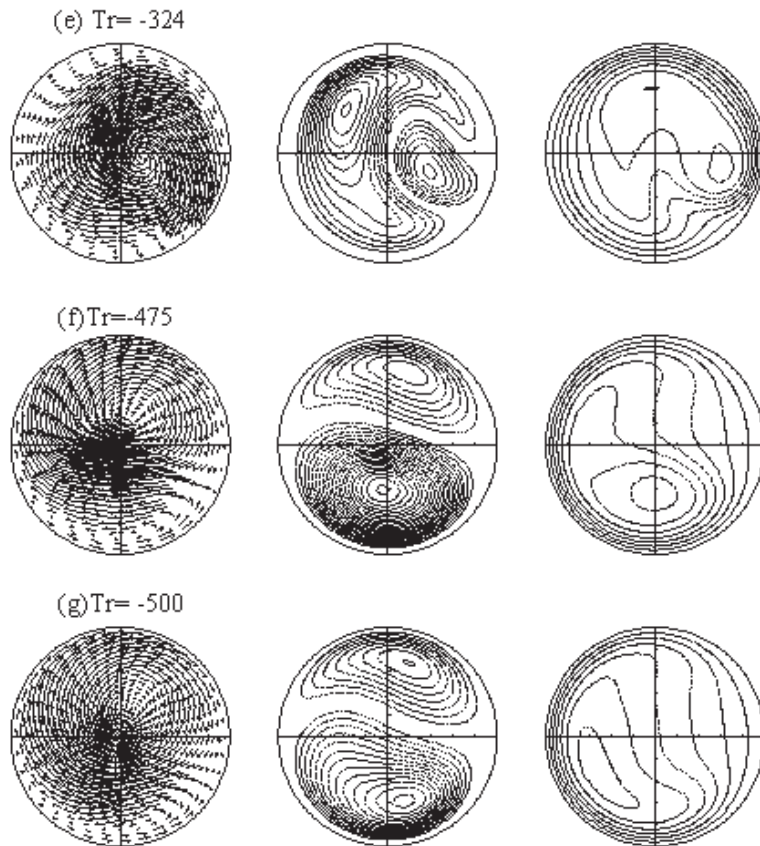


FIG. 5. (e–g) Vector plots of the secondary flow (left), stream-lines of the secondary flow (middle) and contour plots of the axial flow (right) through the rotating helical pipe at different values of Tr in case of $D_n = 2000$, with $\beta_0 = 0.4$ and $\delta = 0.01$.

6. Conclusions

1. Many solutions have not been obtained in case of a rotating helical pipe with circular cross-section.
2. The single cell with minor cell structure of the secondary flow at the maximum flux appears in case of Dean number 1500 and 2000. Similar flow behaviours are observed after and before the peak point.
3. Near the maximum flux point, the strength of the vectors of the secondary velocity is fairly weak and very weak near the periphery of the cross-section. This may be due to the weak effect of interaction of the centrifugal force with the Coriolis force.

References

1. BERGER S.A. and TALBOT L., *Flow in curved pipes*, Ann. Rev. Fluid Mechanics, **15**, 461–512, 1983.
2. Chen, W.H. and FAN C.N., *Finite element analysis of incompressible viscous flow in a helical pipe*, Computational Mechanics, **1**, 281–292, 1986.
3. CHEN W. and JAN R., The characteristics of Laminar flow in a helical circular pipe, Journal of Fluid Mechanics, **244**, 241–256, 1992.
4. DASKOPOULOS P. and LENHOFF A.M., *Flow in curved ducts: bifurcation structure for stationary ducts*, Journal of Fluid Mechanics, **203**, 125–148, 1989.
5. DASKOPOULOS P. and LENHOFF A.M., *Flow in curved ducts: Part 2. Rotating ducts*, Journal of Fluid Mechanics, **217**, 575–593, 1990.
6. DEAN W.R., *Note on the Motion of Fluid in a Curved Pipe*, Philosophical Magazine and Journal of Science, **4**, 20, 208–223, 1927.
7. GERMANO M., *On the effect of torsion on a helical pipe flow*, Journal of Fluid Mechanics, **125**, 1–8, 1982.
8. GERMANO M., *The Dean equations extended to a helical pipe flow*, Journal of Fluid Mechanics, **203**, 289–305, 1989.
9. ITO H., *Secondary flow in rotating curved pipe*, The reports of the Institute of High Speed Mechanics, Tohoku University, Sendai, Japan, **29**, 270, 33–57, 1974.
10. ITO H., *Flow in curved pipes*, JSME International Journal, **30**, 262, 543–552, 1987.
11. ISHIGAKI H., *Analogy between laminar flows in curved pipes and orthogonally rotating pipes*, Journal of Fluid Mechanics, **268**, 133–145, 1994.
12. KAO H.C., *Torsion effect on fully developed flow in a helical pipe*, Journal of Fluid Mechanics, **184**, 335–356, 1987.
13. LIU S. and MASLIYAH J.H., *Axially invariant laminar flow in helical pipes with a finite pitch*, Journal of Fluid Mechanics, 251, 315–353, 1993.
14. MANLAPAZ R.L. and CHURCHILL S.W., *Fully developed laminar flow in a helically coiled tube of finite pitch*, Chemical Engineering Communications, **7**, 57–78, 1993, 1980.
15. MIYAZAKI H., *Combined free- and forced-convective heat transfer and fluid flow in rotating curved circular tube*, International Journal of Heat and Mass Transfer, **14**, 1295–1309, 1971.
16. MURATA S. MIYAKE, Y., INABA T. and OGAWA H., *Laminar flow in a helically coiled pipe*, Bulletin of the JSME, **24**, 355–362, 1981.
17. NANDAKUMAR K. and MASLIYAH J.H., *Bifurcation in steady laminar flow through curved tubes*, Journal of Fluid Mechanics, **119**, 475–490, 1982.
18. TUTTLE E.R., *Laminar flow in twisted pipes*, Journal of Fluid Mechanics, 219, 545–570, 1990.
19. XIE D.E., *Torsion effect on secondary flow in a helical pipe*, International Journal of Heat and Fluid Flow, **11**, 114–119, 1990.

20. WANG C.Y., *On the low-Reynolds-number flow in a helical pipe*, Journal of Fluid Mechanics, **108**, 185–194, 1981.
21. YANASE S., YAMAMOTO K. and YOSHIDA T., *Effect of curvature on dual solutions of flow through a curved circular pipe*, Fluid Dynamics Research, **13**, 217–228, 1994.
22. YAMAMOTO K., YANASE S. and YOSHIDA T., *Torsion effect on the in a helical pipe*, Fluid Dynamics Research, **14**, 259–273, 1994.
23. YAMAMOTO K., AKITA T., IKEUCHI H. and KITA Y., *Experimental study of the flow in a helical circular tube*, Fluid Dynamics Research, **16**, 237–249, 1995.
24. YAMAMOTO K., MAHMUD ALAM, JUNICH YASUHARA and AGUS ARIBOWO, *Flow through a rotating helical pipe with circular cross-section*, International Journal of Heat and Fluid Flow, **21**, 213–220, 2000.

Received September 29, 2006; revised version May 13, 2007.
